Division of Informatics, University of Edinburgh

Institute of Perception, Action and Behaviour

Faithful recovering of quadric surfaces from 3D range data

by

Naoufel Werghi, Robert Fisher, Anthony Ashbrook, Craig Robertson

Informatics Research Report EDI-INF-RR-0089

Division of Informatics **October 1999**
http://www.informatics.ed.ac.uk/

Faithful recovering of quadric surfaces from 3D range data

Naoufel Werghi, Robert Fisher, Anthony Ashbrook, Craig Robertson

Informatics Research Report EDI-INF-RR-0089

DIVISION *of* INFORMATICS
Institute of Perception, Action and Behaviour

October 1999

Proc. 2nd Int. Conf. on 3-D Digital Imaging and Modeling, Ottawa, Canada, pp 280-289, October 1999.

Abstract :

Keywords :

Faithful recovering of quadric surfaces from 3D range data

N.Werghi R.B. Fisher, A. Ashbrook, C. Robertson
Institute of Perception Action and Behaviour
Division of Informatics
University of Edinburgh
Edinburgh, UK
{naoufelw, rbf, anthonya, craigr}@dai.ed.ac.uk

Abstract

The paper proposes a reliable method for estimating quadric surfaces from 3D range data in the framework of object recognition and localization or object modelling. Instead of estimating a quadric surface individually the approach fits all the surfaces captured in the scene together taking into account the geometric relationships between them and their specific characteristics. The technique is compared with other methods through experiments performed on real objects.

1. Introduction

Common quadric surfaces such as cylinders, cones and spheres are found in most manufactured parts and objects. A reliable estimation of these surfaces is an essential requirement in object modelling or reverse engineering, where a faithful model is needed to be extracted from the set of range data for CAD/CAM purposes.

One obstacle to achieving this goal is the inaccuracy of shape estimates from the extracted quadric patches. This arises from the limited field of the sensor which can only cover a partial area of an object in a given view, self or external occlusion of the object and finally some surface data may be lost during the surface segmentation process either due to segmentation failure or intentionally in order to avoid unreliable data. The usable set of data points may thus represent only a small area of the surface (Figure 1) and consequently give unstable estimates of the surface shape. Furthermore the remaining available data is corrupted by measurement noise. Consequently the surface fitting fails to give a reliable estimation of the surface shape. The estimates are highly biased and may not reflect the actual type of the surface even when sophisticated techniques are applied.

The idea presented here is to compensate the poorness of information embodied in the quadric surface data by extra knowledge about the surface such as the surface type and relationships with other nearby surfaces. This additional information is either provided by the model in the case of model-based applications or deduced from a set of potential hypotheses generated, checked and verified within a perceptual organization process. E.g if preliminary estimates of a cylinder and plane lead to an angle between the plane normal and the cylinder axis close to 90^o, it is very likely that the two surfaces are orthogonal, or if the estimated shape of a quadric is an elliptic cylinder with major axis and minor axis having nearly identical values it is very likely that the

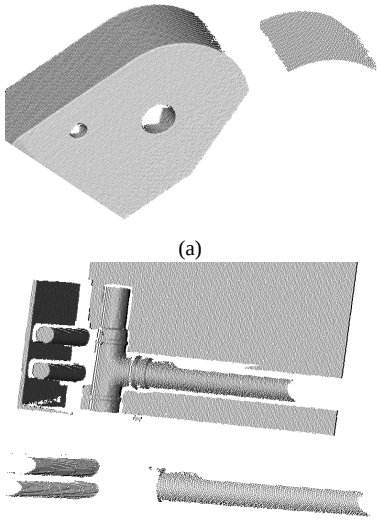

(a) (b)

Figure 1. (a) Object containing a cylindrical surface, only a small area of of the cylinder surface is visible. (b) A miniaturised model of a plant: because of the noise and the segmentation errors, only small portions of the pipes are extracted and can be used reliably for the estimation.

cylinder is circular.

The exploitation of this extra information is quite feasible since a patch is rarely captured alone in the scene but rather with close or adjacent surfaces which could be either planes or quadrics.

This paper shows how the extra information can be represented in a shape estimation process and then evaluates the approach against several alternatives, concluding that the extra information is both effective and easy to exploit.

2. Problem statement and previous work

A quadric surface S is represented by the implicit function:

$$f(x,y,z,\vec{p}) = ax^2 + by^2 + cz^2 + 2hxy + 2gxz + 2fyz + 2ux + 2vy + 2wz + d = 0 \quad (1)$$

Given a set of N measurement points X_i we want to find the parameter vector $\vec{p} = [a,b,c,h,g,f,u,v,w,d]$ such that the function defined by (1) reflects as well as possible the actual shape of the surface. The type and shape characteristics of the surface are deduced afterwards from $\vec{p}$.

A reasonable criterion to judge the goodness of the solution is the sum of the squared Euclidean distances between each measurement point and the surface, $J = \sum_{i=1}^{N} d(X_i,S)^2$. The parameter vector minimizing this criterion is the best solution in the least squares sense. Unfortunately the non-linearity of this distance measure does not lead to a nice and easy closed-form solution for the parameter vector $\vec{p}$. Various approximations of this distance have been therefore proposed in the literature to make the minimization problem easier.

The most common one is using the value of the implicit function $f(x,y,z)$ known as the algebraic distance. It has been used in recovering planes and quadrics [3, 6]. Although this approximation is highly attractive because of its closed-form solution, it was subject to many criticisms since it leads to a highly biased estimation for small surfaces with low curvature. An improved approximation was suggested by expanding the implicit function into Taylor's series up to first or second degree. The first approximation is given by:

$$\frac{f(x,y,z)^2}{\|\vec{\nabla} f(x,y,z)\|^2} \quad (2)$$

Taubin [13] noted that for the surfaces with constant gradient the estimation based on the first approximation is the solution of a generalized eigenvalue problem:

$$H\vec{p} = \lambda DH\vec{p} \quad (3)$$

where

$$H = \sum_i \vec{h_i}\vec{h_i}^T \quad (4)$$

$$DH = \sum_i dh_i dh_i^T \quad (5)$$

$$\vec{h_i} = [x_i^2, y_i^2, \cdots, 1]^T \quad (6)$$

and dh_i is the Jacobian matrix of h_i with respect to $[x_i, y_i, z_i]$.

Other than this case the problem is a non-linear minimization which needs to be solved iteratively, e.g the algorithm proposed by Kumar *et al* [8] for fitting Hyperquadric surfaces. When the gradient of the surface vanishes, the first approximation is no longer valid. To avoid this singularity problem Taubin [14] introduces a high order approximate distance and estimates the solution with a non-linear fitting procedure. Lei and Cooper [9] used both the first and second approximation for fitting 2D curves but they convert the minimization problem to linear programming optimization by using the measurements points as control points constraining the shape of the curve. Sullivan *et al* [12] minimized the sum of the exact geometric distances and consider the implicit function representing the surface as a constraint function. They solved the problem with an iterative algorithm combining Levenberg-Marquardt technique and Newton method.

Recently Luckács *et al* [10] consider an approximation of geometric distance specific to each quadric type, namely, sphere, cylinder, cone, and torus. The algorithm ensures stable and faithful estimation.

Another way for considering the Euclidean distance is to use a specific representation function for a particular case of quadric surfaces, like the circular cylinder, circular cone and sphere. A circular cylinder can be defined by:

$$(x-x_0)^2 + (y-y_0)^2 + (z-z_0)^2 - (n_x(x-x_0) + n_y(y-y_0) + n_z(z-z_o))^2 - r^2 = 0 \quad (7)$$

where $\vec{X_o} = [x_0, y_0, z_0]^T$ is an arbitrary point on the axis, $\vec{n} = [n_x, n_z, n_y]^T$ is a unit vector along the axis and r is the radius of the cylinder. A circular cone can be represented by:

$$[(x-x_o)^2 + (y-y_o)^2 + (z-z_o)^2]cos^2(\alpha) - [n_x(x-x_o) + n_y(y-y_o) + n_z(z-z_o)]^2 = 0 \quad (8)$$

where $[x_o, y_o, z_o]^T$ is the apex of the cone, $[n_x, n_y, n_z]^T$ is the unit vector defining the orientation of the cone axis and α is the semi-vertical angle. A sphere can be defined by:

$$(x-x_0)^2 + (y-y_0)^2 + (z-z_0)^2 - r^2 = 0 \quad (9)$$

where $[x_o, y_o, z_o]^T$ is the centre of the sphere and r is its radius.

With this representation the value of the function at a given point corresponds to the squared Euclidean distance between the point and the surface. This representation and

a slightly different one (replacing the orientation vector by two angles) were used respectively in [1, 5]. In both works the solution was found with a non-linear optimization. The computation cost is dramatically high with this representation. In the case of the cylinder for instance, the computation of the least squares error for N measurement points needs to evaluates and sum the expression (7) N times in each iteration of the optimization algorithm. Whereas with the general expression (1) of the quadric, the least squares error is determined in one single operation, $\vec{p}^T\mathcal{H}\vec{p}$ where $\vec{p}^T = [a, b, ., ., d]$ and H is the data matrix determined with the expression (4). This matrix is computed off-line before the optimization.

A common characteristic of these works is that they treated each single surface individually. When the quadric patch to be fitted covers a small amount of the surface, the fitting technique fails to give a reasonable estimation and often the estimates are highly biased. This is expected since second order functions can easily trade-off curvature and position to produce similar error measures. Thus small patches do not provide sufficient extent to distinguish between the two cases.

However if we place ourselves in an object recognition and localization framework we usually have to fit many surfaces belonging to the same object and which are linked by some geometrical and topological relationships. By exploiting this knowledge together with the information which may be available about the quadric type and shape we hope compensate the lack of information in the quadric patch and obtain therefore a surface parameterization as accurate as possible.

We will show that by a simple representation of the extra information and with a rigorous integration of this information in the fitting process and by using just the algebraic distance the proposed approach makes a good trade-off between estimation accuracy and computational cost.

3. Principle of the approach

Consider a set of M surface patches of an object extracted from a given view. We assume that the set may contain quadric and planar patches. By considering the algebraic distance the minimization criterion related to the surface k has the form

$$J_k = \sum_{i=1}^{N_k} f(x_i, y_i, z_i, \vec{p_k})^2 \tag{10}$$

for N_k data points $(x_i, y_i, z_i)^T$ lying on the surface. This expression can be put into the form

$$J_k = \vec{p_k}^T \mathcal{H}_k \vec{p_k} \tag{11}$$

where $\vec{p_k}$ is the parameter vector and H_k is a nonnegative, definite and symmetric matrix:

$$H_k = \sum_{i=1}^{N_k} \vec{h_i}\vec{h_i}^T \tag{12}$$

$\vec{h}$ is a measurement vector function of the measurement point (x, y, z). E.g for a plane and a quadric, $\vec{h}$ is defined respectively by:

$$\vec{h} = [x, y, z, 1]^T \tag{13}$$

$$\vec{h} = [x^2, y^2, z^2, 2xy, 2xz, 2yz, 2x, 2y, 2z, 1]^T \tag{14}$$

A global minimization criterion for all the surfaces is the sum of all the single criterions

$$\begin{aligned} J &= J_1 + J_2 + \cdots + J_M \\ &= \vec{p}^T\mathcal{H}\vec{p} \end{aligned} \tag{15}$$

where $\vec{p}$ is a global parameter vector concatenating all the single parameter vectors and $\mathcal{H}$ is a global data matrix containing the set of matrices $\mathcal{H}_k$. $\mathcal{H}$ is nonnegative, definite and symmetric as well. For example consider an object with two surfaces, a plane and a quadric. Let H_{plane} and $H_{quadric}$ their associated data matrices. The matrix $\mathcal{H}$ will have the following structure:

$$\mathcal{H} = \begin{bmatrix} (H_{plane})_{4,4} & (O)_{(4,10)} \\ (O)_{(10,4)} & (H_{quadric})_{(10,10)} \end{bmatrix}$$

The relationships between the different surfaces as well as the shape characteristics of the surfaces are formulated into a set of vector functions

$$C_j(\vec{p}), \quad j = 1..K \tag{16}$$

Examples of these functions are given in Section 5. So the problem can be seen as a constrained optimization problem where we have determine the parameter vector $\vec{p}$ minimizing (15) subject to the constraints (16). As we will see with the test objects, most of the constraint functions are non-linear making the development of a closed form solution or the application of a linear programming techniques quite hard or impossible. The problem belongs to the category of quadratic objective function with non-linear constraints. These problems are well behaved if the constraint functions are continuous, differentiable and convex [4]. We propose a matrix formulation of the relationships and the shape characteristics which satisfies these requirements. Furthermore this representation ensures compact form and avoids expressions with many variables.

The estimation of the parameter vector is achieved with a sequential unconstrained technique [15]. We consider the following optimization function

$$E(\vec{p}) = \vec{p}^T\mathcal{H}\vec{p} + \sum_{k=1}^{K} \lambda_k C_k(\vec{p}) \tag{17}$$

where the second term is a penalty function consisting of the sum of squared constraint functions weighted each by a positive value λ_k. The algorithm increments sequentially the set of weights and at each step (17) is minimized with the standard Levenberg-Marquardt technique and the vector $\vec{p}$ is updated. The algorithm stops when the constraints are satisfied to the desired degree or when the parameter vector remains stable for a certain number of iterations. When λ_k becomes large, the Hessian matrix invloved in Levenberg-Marquardt may become ill-conditioned and consequently its inversion may cause numerical instabilities. To overcome this problem we perform the inversion in different steps following the method developed by Broyden *et al* [2]. The initial parameter $\vec{p}_o$ is determined by estimating each surface individually with a generalized eigenvalue technique [3] and then concatenating all the vectors into a single one.

4. Parametrization of the cylinder, the cone and the sphere

When the treated object contains planes and quadrics the relationships between a quadric surface and other surfaces are relative orientation and relative position for cylinders and cones and relative position for spheres. The circularity of a cylinder or a cone is additional knowledge about the quadric shape which should be taken into account as well.

Unfortunately the coefficients of the implicit function (1) do not have obvious geometric significance. Formulating the geometric relationships only with these parameters leads to complex constraint function often with singular cases. To avoid this problem, we introduce the orientation of the quadric axis defined by a normal vector $[n_x, n_y, n_z]^T$ as additive parameters for the cylinder and the cone. Each of these two surfaces will be defined then by the following parameter vector:

$$[a, b, c, h, g, f, u, v, w, d, n_x, n_y, n_z]^T \qquad (18)$$

This representation over-parameterizes the quadric; in return it allows a simple formulation of the geometric relationships between cone, cylinder and other surfaces, e.g. the relative orientation between a plane and a quadric is expressed by

$$\vec{n_q}^T \vec{n_p} - cos(\alpha) = 0; \qquad (19)$$

where α is the angle between the plane's normal and the quadric axis, $\vec{n_q}$ and $\vec{n_p}$ are the quadric axis orientation and the plane normal respectively.

Based on the above parametrization the circularity of the cylinder is expressed by the following equations

$$\begin{array}{lllllll} a & = & 1 - n_x^2 & & h & = & -n_x n_y \\ b & = & 1 - n_y^2 & & g & = & -n_x n_z \\ c & = & 1 - n_z^2 & & f & = & -n_y n_z \end{array} \qquad (20)$$

and for the cone by:

$$\begin{array}{lllllll} a - b & = & n_x^2 - n_y^2 & & h & = & n_x n_y \\ a - c & = & n_x^2 - n_z^2 & & g & = & n_x n_z \\ b - c & = & n_y^2 - n_z^2 & & f & = & n_y n_z \end{array} \qquad (21)$$

These relations are obtained by expanding the equations (7) and (8) and identifying with the general quadric equation (1).

A sphere is characterized by equal coefficients for the x^2, y^2 and z^2 terms and vanishing coefficients for the cross products terms. Its representation is:

$$a(x^2 + y^2 + z^2) + 2ux + 2vy + 2wz + d = 0 \qquad (22)$$

5. Experiments

A series of experiments were performed on several real objects having planar and quadric surfaces. The segmentation and the extraction of the surfaces were performed with *rangeseg* [7].

Our approach were compared with three main techniques covering a large part of the spectrum of the fitting techniques developed in the literature. These techniques are the eigenvalues solution based on the algebraic distance [3, 6], the eigenvalue technique [13] based on the approximation of the Euclidean distance (2) and the iterative optimization technique [1, 5] based on the specific representations of quadric (7), (8) and (9), in occurrence the circular cone, the circular cylinder and the sphere. In the rest of the paper these techniques will be referenced respectively by AD, AED, SR and the new suggested global fitting approach by GF.

The performances of the different techniques are evaluated by comparing the shape parameters of the quadrics, for instance the half angle for the cone and the radius for the cylinder and the sphere. The computation time was taken into account as well. With AD, and AED the estimation time is almost instantaneous, whereas it varies from half an hour to several hours for the SR depending on the number of measurement points. For the GF technique it is in the range of minutes. The different techniques were implemented in Matlab on a shared system of a 200 MHz Sun Ultrasparc workstation. The GF has been also implemented in C++, the package contains an additional module for compiling the constraints. The computation time is still in the order of minutes. It is expected to be highly reduced on a dedicated system However.

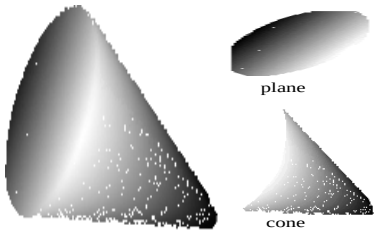

Figure 2. the cone object and the extracted surfaces.

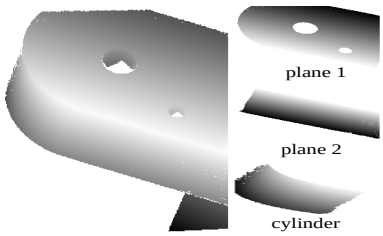

Figure 3. a view of object 2 with the extracted surfaces.

5.1. Object 1

Consider object 1 composed of a cone and a plane base (Fig.2). The axis of the cone is perpendicular to the plane. This constraint is imposed by associating a single normal vector to both the orientation of the cone axis and the plane's normal. The object is then represented by the parameter vector:

$$\vec{p} = [a, b, c, h, g, f, u, v, w, d, n_x, n_y, n_z, l]$$

where l is the distance parameter of the plane. The mininization criterion is:

$$J = \vec{p}^T \mathcal{H} \vec{p}, \quad \mathcal{H} = \begin{bmatrix} H_{cone} & (O) \\ (O) & H_{plane} \end{bmatrix}$$

where H_{cone} and H_{plane} are the data matrices defined in (12) of the cone surface and the plane surface respectively. The constraint function associated to the circularity of the cone is deduced from (21) and by using a vector function formulation the penalty function associated to this shape constraint is

$$C_{circ}(\vec{p}) = \sum_{i=1}^{6} (\vec{v_i}^T \vec{p} - \vec{p}^T A_i \vec{p})^2$$

where $\vec{v_i}$ and A_i are appropriate vectors and matrices (see [15] for more details). To ensure the unity of the normal vector $[n_x, n_y, n_z]^T$ we introduce the penalty function:

$$C_{unit}(\vec{p}) = (\vec{p}^T U \vec{p} - 1)^2$$

where U is an appropriate matrix. The optimization function (17) is thus set up as follows:

$$\vec{p}^T \mathcal{H} \vec{p} + \lambda_1 C_{unit}(\vec{p}) + \lambda_2 C_{circ}(\vec{p})$$

The results obtained with the different techniques are grouped in Table 1 except for the AED technique since a cone surface does not have a constant gradient value. The AD technique gives an elliptic cone, whereas the SR and GF ensures a faithful shape estimate and relatively better accuracy with the GF. The computation time for the SR is in the order of 30 min whereas it is 2 min for the GF.

5.2. Object 2

In the view shown in Figure 3, a small part of the cylinder surface is visible (about 20%) of a whole cylinder. The cylinder is circular and its axis is orthogonal to plane 1 and parallel to plane 2. The constraint functions were deduced from (19) and (20) and then considered in the fitting technique. Table 2 summarizes the results. The SR fitting took 40 min whereas the GF took only 3mn.

5.3. Object 3

The cylinder patch is extracted from the view shown in Figure 4 with two other plane surfaces. The axis of the cylinder patch is parallel to plane 1 and orthogonal to plane 2. The cylinder is circular and the extracted patch covers less than half cylinder. The computation time is 25 min for the SR and 3min for GF The results are grouped in Table 3.

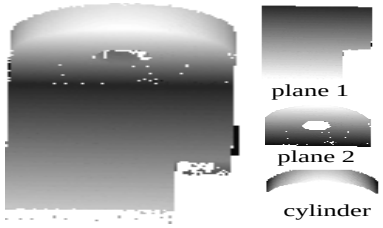

Figure 4. View of object 3 with the extracted surfaces.

5.4. Object 4

This object contains a half cylinder with four plane surfaces. The cylinder patch covering about 20% of the whole cylinder and was extracted with two other visible planes. The considered relationships are the orthogonality of the cylinder axis to plane 1 and its inclusion in plane 2. The circularity of the cylinder was included as well. The fitting time is about 1 hour and a half with the SR and 4 min with GF. The results of the fitting are presented in Table 4.

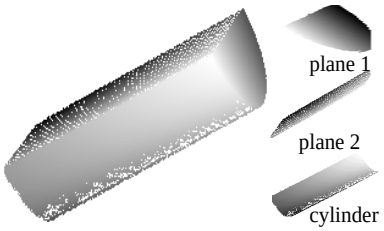

Figure 5. View of object 4 with the extracted surfaces.

5.5. Object 5

This object is a miniaturized plant model. Two cylinders and two planes were extracted from the view shown in Figure 6. Cylinder 1 and cylinder 2 are orthogonal respectively to plane 1 and plane 2. They are also mutually orthogonal and circular. The computation time with SR is about 30 min for each cylinder and 5min with GF. The different estimates are presented in Table 5.

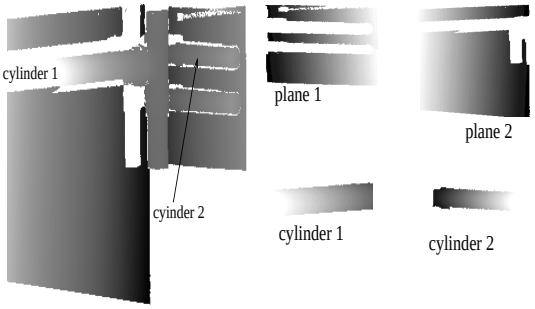

Figure 6. View of object 5 with the extracted surfaces.

5.6. Object 6

This object (Fig.7) contains a circular cone and a circular cylinder having perpendicular axes. The cylindrical patch covers nearly 20% of the whole cylinder and the cone patch around 30 %. We have not considered the relationships between the two lateral planes and the quadric surfaces but they can be also integrated without any particular difficulty. Since the patches contain a large amount of data points (nearly 25000 and 7000 points for the cylinder and the cone respectively) the SR fitting is quite high time consuming, about six hours for the cylinder and around two hours for the cone. With the GF the two surfaces are simultaneously estimated in 5 min. The different estimates are summarized in Table 6.

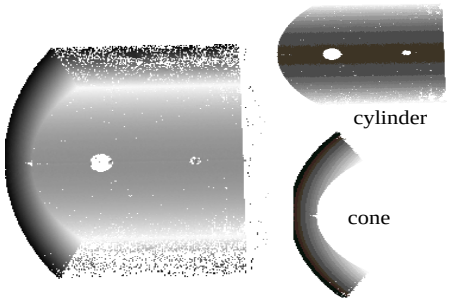

Figure 7. View of object 6 with the extracted surfaces.

5.7. Object 7

This object contains a circular cylinder and a half sphere. The two surfaces have the same radius and the axis of the cylinder goes through the centre of the sphere. In the view shown in Figure 8 a nearly quarter of sphere and half cylinder are visible. The SR fitting time is two hours for the cylinder and 20 min for the sphere. With the GF it is 4 min. The estimates are shown in Table 7.

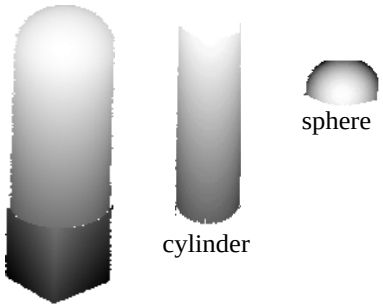

Figure 8. View of object 7 with the extracted surfaces.

6. Discussion and Conclusion

It is clearly noticed from the different tables related to objects having circular cones or circular cylinders that when the shape of the quadric is not constrained the AD and AED algorithms do not guarantee a faithful shape estimation. Both techniques result in elliptic cones or elliptic cylinders with a bias more or less important depending on how much the patch covers the quadric and the number of measurement points in each patch. However the AED technique estimates are less biased. Figure 9 illustrates the difference where the bias in the shape estimates is expressed in terms of the (minor axis/major axis) ratio. The same aspect is noticed for the cones if we compare the cone estimates for object 1 (Table 1) and object 6 (Table 6).

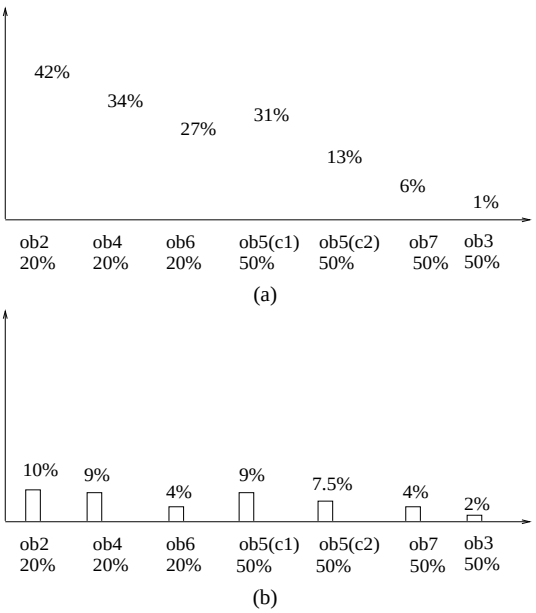

Figure 9. shape bias in the cylinder estimates (ob:object, c1:cylinder1,etc.). (a) with the AD technique, (b) with the AED technique

By imposing the circularity constraint the SR and the GF give faithful estimates in terms of shape and parameter values. It is noticed however that the results are usually more accurate with the GF. This suggested that by taking into account the different position and orientation relationships constraining the location of the quadric surface the estimate is greatly improved. When a specific algebraic function is used for the sphere (22) all the techniques give accurate estimates (Table 7).

The computation time is dramatically high with the SR technique, and may take hours for surface with large amounts of data. This is normal with this non-linear representation where the data terms can not be grouped and cumulated separately. In the GF approach, the measurement data are computed and encapsulated in a data matrix just once prior to the optimization process. Consequently the computation time is virtually independent of the amount of data points and is kept in the range of minutes.

Although it is not the objective of this work we believe that the consideration of all the known relationships between the quadric surface and other surfaces very likely shifts the position of the surfaces towards the actual one in the sense that incorporating these constraints may compensate up to certain degree for the effects of systematic errors. This aspect was mentioned in [1] for the circularity of the quadric. Generalizing this aspect for geometric relationships between surfaces can be a worthwhile future work.

The optimization technique used in the GF algorithms supposes a reasonable initialisation of the surface parameter vector. Although this condition limits the field of application of the technique, it is well satisfied in our framework. We propose to use the estimates given by the AD or when possible the AED as initialization. More generally we suggest the scheme illustrated in Figure 10 for optimal combination of the AD, AED and the GF for the estimation of object surfaces.

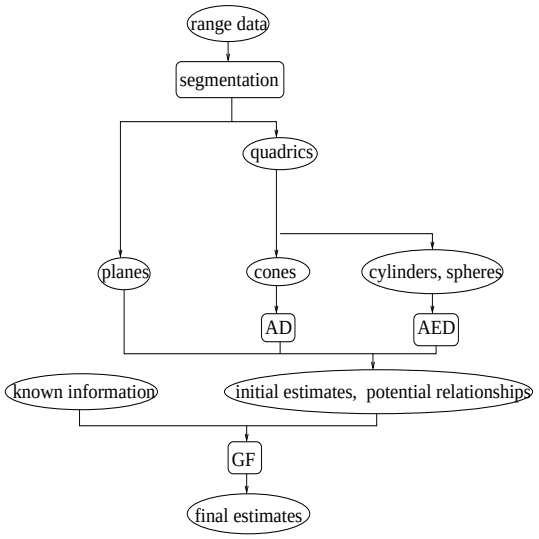

Figure 10. General scheme for object surfaces estimation.

Acknowledgements

The work presented in this paper was funded by UK EPSRC grant GR /L25110.

AD	AED	SR	GF	true surface
ell.cone:	-	cir.cone	cir.cone	cir.cone
$\alpha_{max} = 21.41^o$	-	$\alpha = 20.77^o$	$\alpha = 19.68^o$	$\alpha = 20^o$
$\alpha_{min} = 20.19^o$	-			

Table 1. Estimates of the cone shape with the different techniques.

AD	AED	SR	GF	true surface
ell.cylinder	ell.cylinder	cir.cylinder	cir.cylinder	cir.cylinder
$r_{max} = 30.41$	$r_{max} = 41.58$	$r = 44.25$	$r = 44.62$	$r = 45$
$r_{min} = 17.50$	$r_{min} = 37.80$			

Table 2. Estimates of the cylinder patch of object 2.

AD	AED	SR	GF	true surface
ell.cylinder	ell.cylinder	cir.cylinder	cir.cylinder	cir.cylinder
$r_{max} = 21.74$	$r_{max} = 24.64$	$r = 20.23$	$r = 20.05$	$r = 20.00$
$r_{min} = 21.42$	$r_{min} = 24.13$			

Table 3. Estimates of the cylinder patch of object 3.

AD	AED	SR	GF	true surface
ell.cylinder	ell.cylinder	cir.cylinder	cir.cylinder	cir.cylinder
$r_{max} = 21.74$	$r_{max} = 28.08$	$r = 29.61$	$r = 29.68$	$r = 30.00$
$r_{min} = 14.19$	$r_{min} = 26.47$			

Table 4. Estimates of the cylinder patch of object 4.

AD	AED	SR	GF	true surface
ell.cylinder	ell.cylinder	cir.cylinder	cir.cylinder	cir.cylinder
$r1_{max} = 17.69$	$r1_{max} = 9.01$	$r1 = 8.08$	$r1 = 7.44$	$r1 = 7.50$
$r1_{min} = 12.12$	$r1_{min} = 8.13$			
$r2_{max} = 4.96$	$r2_{max} = 5.67$	$r2 = 5.23$	$r2 = 4.95$	$r2 = 5.00$
$r2_{min} = 4.28$	$r2_{min} = 5.24$			

Table 5. Estimates of the cylinder patches of object 5.

AD	AED	SR	GF	true surface
ell.cylinder	ell.cylinder	cir.cylinder	cir.cylinder	cir.cylinder
$r_{max} = 46.10$	$r_{max} = 57.62$	$r = 59.81$	$r = 59.54$	$r1 = 60$
$r_{min} = 33.66$	$r_{min} = 55.42$			
ell.cone	-	cir.cone	cir.cone	cir.cone
$\alpha_{max} = 28.86^o$	-	$\alpha = 26.84^o$	$\alpha = 31.80^o$	$\alpha = 30^o$
$\alpha_{min} = 25.19^o$	-			

Table 6. Estimates of the cylinder and the cone patches of object 6.

AD	AED	SR	GF	true surface
ell.cylinder	ell.cylinder	cir.cylinder	cir.cylinder	cir.cylinder
$r_{max} = 14.46$	$r_{max} = 14.64$	$r = 14.98$	$r = 14.95$	$r = 15.00$
$r_{min} = 13.51$	$r_{min} = 14.01$			
sphere	sphere	sphere	sphere	sphere
r=15.03	r=15.05	15.03	15.03	15.00

Table 7. Estimates of the cylinder and the sphere patches of object 7.

References

[1] R.M.Bolle, D.B.Cooper, *On Optimally Combining Pieces of Information, with Application to Estimating 3-D Complex-Object Position from Range Data*, IEEE Trans. PAMI, Vol.8, No.5, pp.619-638, September 1986.

[2] C.G Broyden, N.F. Attia, *Penalty Functions, Newton's Method and Quadratic Programming*, Journal of optimization theory and applications, Vol.58, No.3, 1988.

[3] O.D.Faugeras and M. Hebert, *The Representation, Recognition and Positioning of 3-D Shapes from Range Data*, in Techniques for 3-D Machine Perception, ed. A. Rosenfeld, North-Holland, Amsterdam, 1986.

[4] R.Fletcher, *Practical Methods of Optimization*, John Wiley & Sons, 1987.

[5] P.J.Flynn, A.K.Jain. *Surface Classification: Hypothesizing and Parameter Estimation*, Proc. IEEE Comp. Soc. CVPR, pp. 261-267. June 1988,

[6] K.T.Gunnarsson, F.B. Prinz. *CAD model-based loacalization of parts in manufacturing*, IEEE Comput., Vol.20, No.8, pp. 66-74, Aug. 1987.

[7] A. Hoover, G. Jean-Baptiste, X. Jiang, P. J. Flynn, H. Bunke, D. Goldgof, K. Bowyer, D. Eggert, A. Fitzgibbon, R. Fisher. *An Experimental Comparison of Range Segmentation Algorithms.* IEEE Trans. PAMI, Vol.18, No.7, pp.673-689, July 1996.

[8] S.Kumar, S.Han, D.Goldgof, K.Boyer. *On Recovering Hyperquadrics from Range data*, IEEE Trans. PAMI, Vol.17, No.11, pp.1079-1083, November 1995.

[9] Z.Lei, D.B Cooper. *Linear Programming Fitting of Implicit Polynomials*, IEEE Trans. PAMI, Vol.20, No.2, pp.212-217, February 1998.

[10] G. Lukacs, A.D. Marshall and R.R. Martin. *Faithful least-squares fitting of spheres, cylinders, cones and tori for reliable segmentation*, Proc. ECCV'98, Vol.1 pp.671-686, Friburg, Germany, June 1998.

[11] V.Pratt, *Direct Least-squares Fitting of Algebraic Surfaces*, Computer Graphics, Vol.21, pp.145-152, 1987

[12] S.Sullivan, L.Sandford, J.Ponce, *Using Geometric Distance Fits for 3-D object Modelling and Recognition*, IEEE Trans. PAMI, Vol. 16, No.12, pp. 1183-1196, December 1994.

[13] G. Taubin, *Estimation of Planar Curves, Surfaces and Nonplanar Space Curves Defined by Implicit Equations with Applications to Edge and Range Image Segmentation.* IEEE Trans. PAMI, Vol.13, No.11, November 1991

[14] G.Taubin, *An Improved Algorithm For Algebraic Curve and Surface Fitting*, Proc. ICCV'93, Berlin, Germany, pp.658-665, May 1993.

[15] N.Werghi, R.B.Fisher, A.Ashbrook, C.Robertson, *Modelling Objects Having Quadric Surfaces Incorporating Geometric Constraints*, Proc. ECCV'98, pp.185-201, Friburg, Germany, June 1998.